# Conductivity, Thermal Measurements, X-ray Investigations, and Phase Diagram of the $Na_2S_2O_7-K_2S_2O_7$ System

**S. B. Rasmussen, K. M. Eriksen,[†] G. Hatem,[‡] F. da Silva,[‡] K. Ståhl,[†] and R. Fehrmann*[,†]**

*Department of Chemistry and Interdisciplinary Research Center for Catalysis (ICAT), Technical University of Denmark, DK-2800 Lyngby, Denmark, and UMR-CNRS, TECSEN, Avenue Escadrille Normandie Niemen, Faculté des Sciences, St Jérôme 13397, Marseille Cedex 20, France*

*Received: October 25, 2000; In Final Form: December 12, 2000*

The $SO_2$ oxidation catalyst solvent system $Na_2S_2O_7-K_2S_2O_7$ has been investigated by conductometric, calorimetric, and X-ray methods. The phase diagram has been constructed from the phase transition temperatures measured for totally 23 different compositions. The results agree well with previous thermal investigations. The phase diagram has been calculated from classical thermodynamics using all transition temperatures, the heat of liquid−liquid mixing obtained for 18 different compositions, and previously measured fundamental thermal data for liquid and solid $Na_2S_2O_7$ and $K_2S_2O_7$. The phase diagram exhibits two eutectics at $X_{K_2S_2O_7}$ equal to 0.4 (mp 615 K) and 0.6 (mp 613 K), respectively, and a maximum at $X_{K_2S_2O_7} = 0.5$ (mp 619 K) corresponding to formation of the compound $NaKS_2O_7$. This was confirmed by XRD measurements and the crystal structure shown by Rietveld refinement to be triclinic, space group *P*-1, with $a = 5.9050(1)$ Å, $b = 7.2011(1)$ Å, $c = 7.4190(1)$ Å, $\alpha = 101.707(1)°$, $\beta = 90.696(1)°$, $\gamma = 94.241(1)°$, and $Z = 2$. The crystal structure of $K_2S_2O_7$ was confirmed and the unknown structure of $Na_2S_2O_7$ was similarly shown to be triclinic, space group *P*-1, with $a = 6.8037(1)$ Å, $b = 6.8265(1)$ Å, $c = 6.7846(1)$ Å, $\alpha = 116.361(1)°$, $\beta = 95.959(1)°$, $\gamma = 84.194(1)°$, and $Z = 2$. It could be excluded that the compound $NaKS_2O_7$ was a simple solid solution of the two compounds of the binary system. The measured conductivities in the liquid region of the 18 different compositions have been fitted to polynomials of the form $k = A(X) + B(X)(T - T_m) + C(X)(T - T_m)^2$, $T_m = 693$ K.

## Introduction

The molten salt−gas system $M_2S_2O_7-V_2O_5/SO_2-O_2-SO_3-N_2$ (M = alkali) represents a realistic model[1] of the industrial catalyst used for production of sulfuric acid, i.e., catalyzing the reaction $SO_2 + {}^1/_2O_2 \rightleftarrows SO_3$. Previously,[2−5] we have investigated the phase diagrams of the binary systems $K_2S_2O_7-V_2O_5$, $Rb_2S_2O_7-V_2O_5$, $Cs_2S_2O_7-V_2O_5$, and $M_2S_2O_7-V_2O_5$ (M = 80% K + 20% Na) and identified compounds and eutectics with importance for the understanding of the catalyst performance and for the systematic improvement of the catalyst. Systems with M = Li or Na have not been investigated by us since their pyrosulfates decompose at the melting point or by addition of $V_2O_5$. In flue gases and in other wet industrial off-gases, the pyrosulfates are partly transformed to hydrogen sulfates due to the reaction $S_2O_7^{2-} + H_2O \rightleftarrows 2HSO_4^-$. Therefore, we have also investigated[6−8] the binary catalyst solvent systems $M_2S_2O_7-MHSO_4$ such as $Na_2S_2O_7-NaHSO_4$, $K_2S_2O_7-KHSO_4$, $Rb_2S_2O_7-RbHSO_4$, and $Cs_2S_2O_7-CsHSO_4$.

The present work on the binary system $K_2S_2O_7-Na_2S_2O_7$ describes our first research effort on the dry mixed cation catalyst solvent systems $M_2S_2O_7-M'_2S_2O_7$ (M and M′ = alkali cations). These systems are of increasing interest since modern industrial oxidation catalysts contain mixtures of different alkali salts, leading to a higher catalytic activity, especially at the desired lower temperatures, i.e., below ∼420 °C. Furthermore, two very disagreeing phase diagrams—deviating up to 70 K for the liquidus temperature—have previously[9−10] been published for the $Na_2S_2O_7-K_2S_2O_7$ system. This has further motivated the present work, where in addition a different method of investigation has been utilized, i.e., conductometry compared to thermal analysis only in the previous investigations.

**TABLE 1: Liquidus Temperatures and Coefficients for Empirical Equations[a] for the Specific Conductivity of Different Compositions of the Molten $Na_2S_2O_7-K_2S_2O_7$ System in the Measured Temperature Range[b]**

| $X_{K_2S_2O_7}$ | $T_{liq}$ (K) | $A$(X) ($\Omega^{-1}$ cm$^{-1}$) | $B$(X) ($10^{-3}$ $\Omega^{-1}$ cm$^{-1}$ deg$^{-1}$) | $C$(X) ($10^{-6}$ $\Omega^{-1}$ cm$^{-1}$ deg$^{-1}$) | SD ($\Omega^{-1}$ cm$^{-1}$) |
|---|---|---|---|---|---|
| 0.0000 | 676 | 0.4443 | 2.920 | −1.941 | 0.0011 |
| 0.1031 | 665 | 0.3971 | 2.678 | 1.055 | 0.0038 |
| 0.2026 | 644 | 0.3862 | 2.725 | −5.047 | 0.0001 |
| 0.3081 | 627 | 0.3254 | 2.364 | 1.742 | 0.0015 |
| 0.3671 | 618 | 0.3133 | 2.301 | 2.057 | 0.0012 |
| 0.4020 | 614 | 0.2862 | 2.156 | 2.442 | 0.0012 |
| 0.4148 | 615 | 0.3007 | 2.249 | 2.325 | 0.0007 |
| 0.4544 | 615 | 0.2765 | 2.174 | 3.551 | 0.0013 |
| 0.4854 | 614 | 0.2704 | 2.099 | 2.929 | 0.0009 |
| 0.4992 | 613 | 0.3051 | 2.250 | 2.894 | 0.0054 |
| 0.5129 | 614 | 0.2652 | 2.069 | 2.961 | 0.0009 |
| 0.5515 | 612 | 0.2695 | 2.108 | 2.997 | 0.0007 |
| 0.5987 | 615 | 0.2667 | 2.106 | 3.134 | 0.0012 |
| 0.6479 | 626 | 0.2617 | 2.063 | 2.801 | 0.0014 |
| 0.7005 | 636 | 0.2553 | 2.175 | 6.532 | 0.0027 |
| 0.8046 | 653 | 0.2578 | 2.008 | 3.594 | 0.0023 |
| 0.8956 | 670 | 0.2556 | 2.023 | 2.030 | 0.0006 |
| 1.0000 | 692 | 0.2340 | 2.048 | −0.718 | 0.0010 |

[a] $\kappa = A(X) + B(X)(T - T_m) + C(X)(T - T_m)^2$, $T_m = 693$ K. [b] Consult Figures 1 and 2 for the highest measuring temperature.

[†] Technical University of Denmark.
[‡] UMR-CNRS.

10.1021/jp0039262 CCC: $20.00 © 2001 American Chemical Society
Published on Web 03/21/2001

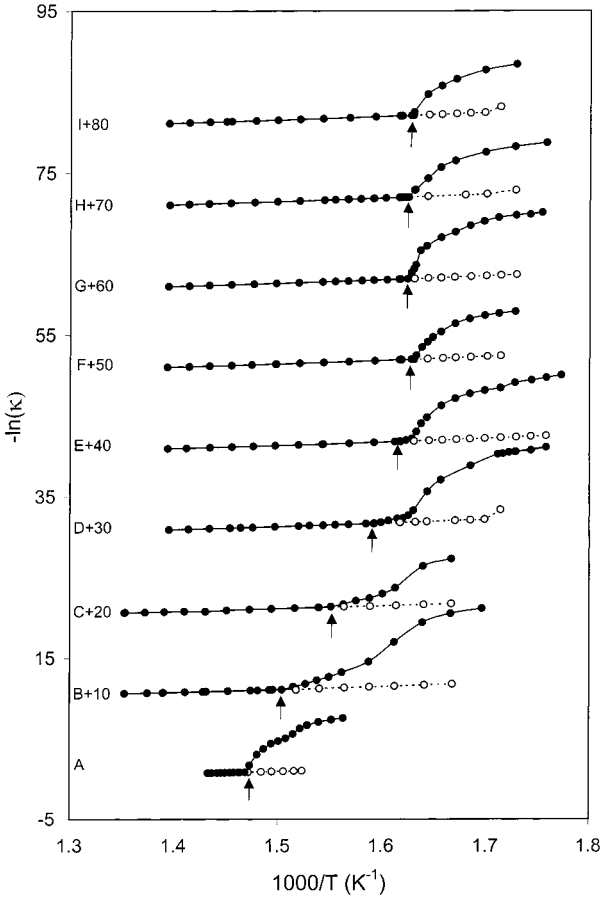


**Figure 1.** Electrical conductivity in the $Na_2S_2O_7-K_2S_2O_7$ system with $-\ln(\kappa)$ vs $1/T$ for the following compositions: A, 0.0000; B, 0.1031; C, 0.2026; D, 0.3081; E, 0.3671; F, 0.4020; G, 0.4148; H, 0.4544, I, 0.4854. For clarity, the data except those for pure $Na_2S_2O_7$ are offset on the ordinate by the specified values. Open circles indicate subcooling.

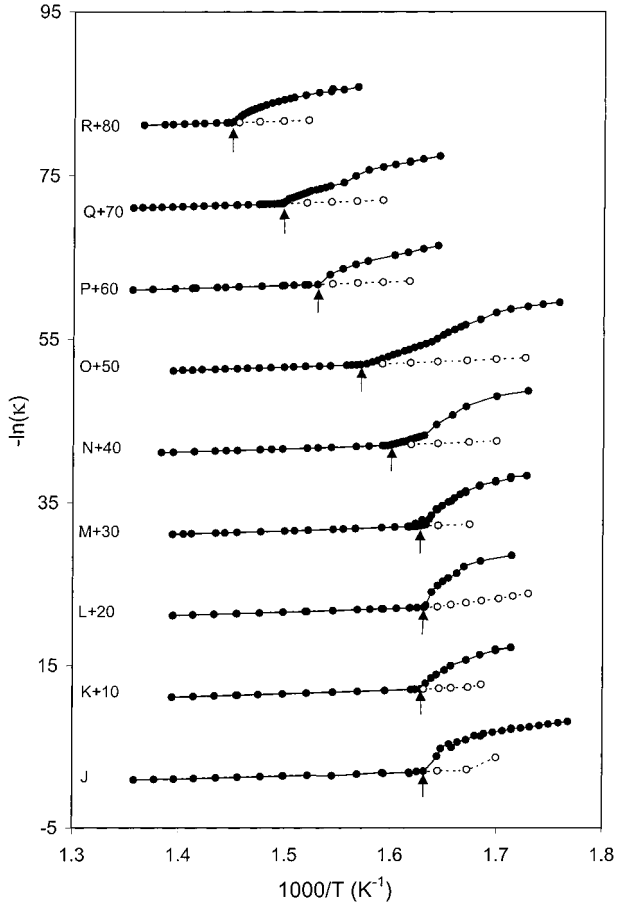


**Figure 2.** Electrical conductivity in the $Na_2S_2O_7-K_2S_2O_7$ system with $-\ln(\kappa)$ vs $1/T$ for the following compositions: J, 0.4992; K, 0.5129; L, 0.5515; M, 0.5987; N, 0.6479; O, 0.7005; P, 0.8046; Q, 0.8956, R, 1.0000. For clarity, the data except those for series J are offset on the ordinate by the specified values. Open circles indicate subcooling.

## Experimental Section

**Chemicals.** The hygroscopic salts $Na_2S_2O_7$ and $K_2S_2O_7$ were prepared by thermal decomposition of, respectively, $Na_2S_2O_8$ and $K_2S_2O_8$ (both Merck, p.a.) in dry $N_2$ atmosphere, as described previously.[11] The salts were kept in sealed ampules, opened and handled only in the drybox.

**Conductivity Measurements.** The electrical conductivity was measured with a borosilicate cell with gold electrodes, sealed vacuum tight into the bottom of the cells as earlier described in detail.[12] The furnace was regulated within ±0.1 °C, and the temperature of the melt was decreased in steps of 5−10 °C until the subcooled melt suddenly crystallized, indicated by a large drop of the electrical conductivity. The temperature was then increased in steps of 0.5−2 °C close to the phase transitions and 5−10 °C far from these transitions until the initial temperature of the melt was reached and the reproducibility of the conductivity checked. The conductivity was measured by a Radiometer CDM-230 conductivity meter, the temperature obtained by cromel−alumel thermocouples calibrated against a Pt100 resistance thermometer, and the cell constants of the order of 100−200 $cm^{-1}$ were found using 0.1 D KCl standard solutions as previously described.[12]

**Thermal Measurements.** Differential enthalpic analysis (DEA) and the partial enthalpies of mixing of $Na_2S_2O_7$ and $K_2S_2O_7$ in the pure salts or binary mixtures were obtained by use of a Calvet micro calorimeter, previously described in detail.[13] The molten salt was contained in a fragile Pyrex ampule and mixed with the melt in the crucible by breaking of the ampule in the melt, at the experimental temperature.

**X-ray Powder Diffraction.** The X-ray powder diffraction data were collected at Beamline I711 of the MAX-II synchrotron in Lund, Sweden.[14] The diffraction patterns were recorded on a Huber G670 powder diffractometer using a wavelength of 1.5226 Å calibrated with Si-standard.[15] The samples were sealed in 0.3 mm capillaries, kept rotating during the 10 min of data accumulation. The data sets were corrected for nonlinearity by a built in calibration routine. An experimentally determined background correction was applied prior to data evaluations, although the original pattern was retained for weighting of the Rietveld refinements.

## Results and Discussion

**Phase Diagram of $Na_2S_2O_7-K_2S_2O_7$.** Eighteen different compositions of the solid and molten $Na_2S_2O_7-K_2S_2O_7$ binary system were investigated by conductometry. The measured temperature ranges were from the completely molten state at 450−470 to 300−350 °C, well below the melting temperature of the eutectics. The results of the measurements are displayed as plots of $-\ln(\kappa)$ vs $1/T$ in Figures 1 and 2. Sharp breaks are observed at the liquidus temperatures, and less marked changes are found at some compositions at the temperature of fusion of the eutectics. For compositions around $X_{K_2S_2O_7} = 0.5$, the liquidus and solidus temperatures are too close to be separated and only one transition temperature can be identified. The

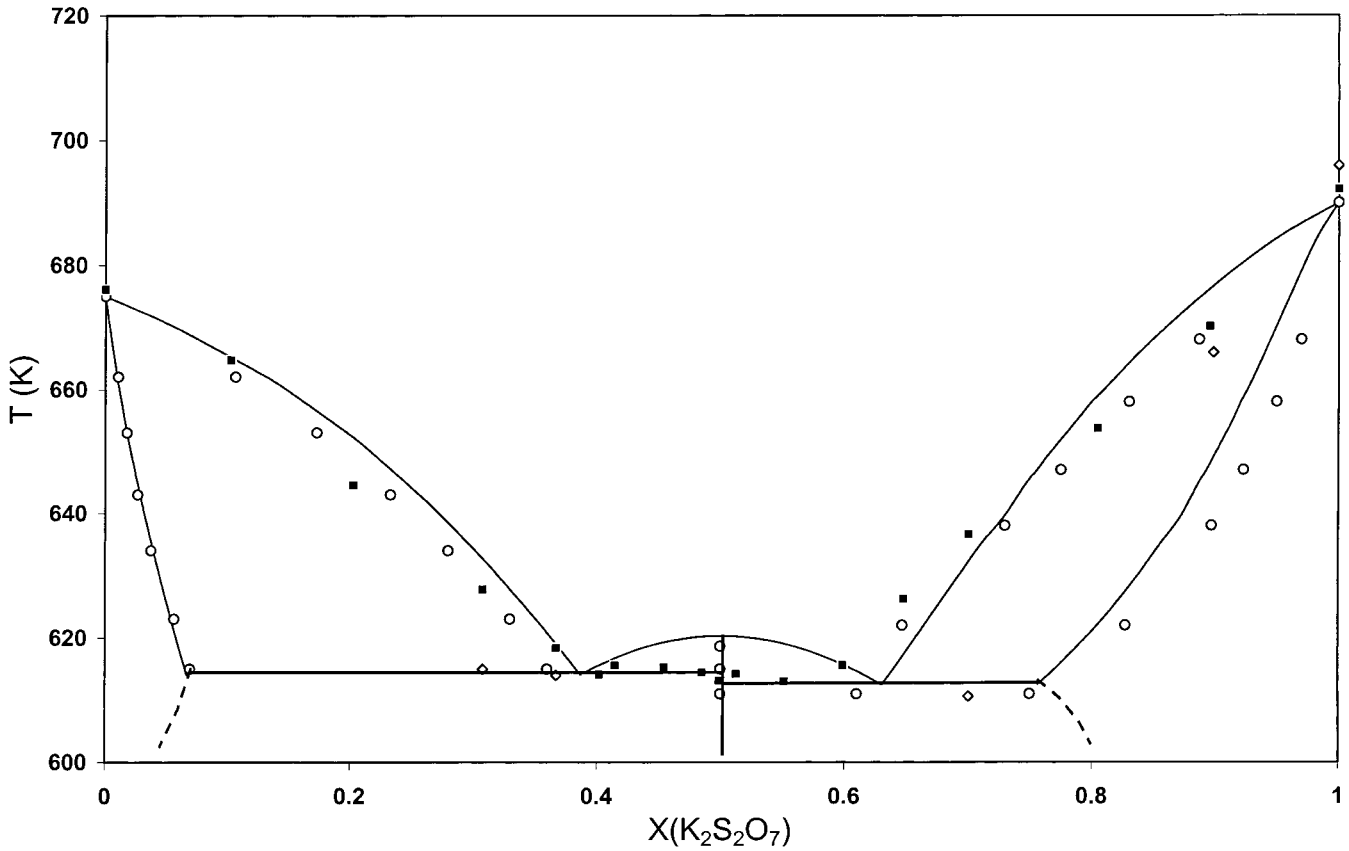


**Figure 3.** Phase diagram of the $Na_2S_2O_7-K_2S_2O_7$ system obtained from conductance (■), DEA (◊), and thermal analysis (○), ref 9. The solid lines have been calculated as described in the text.

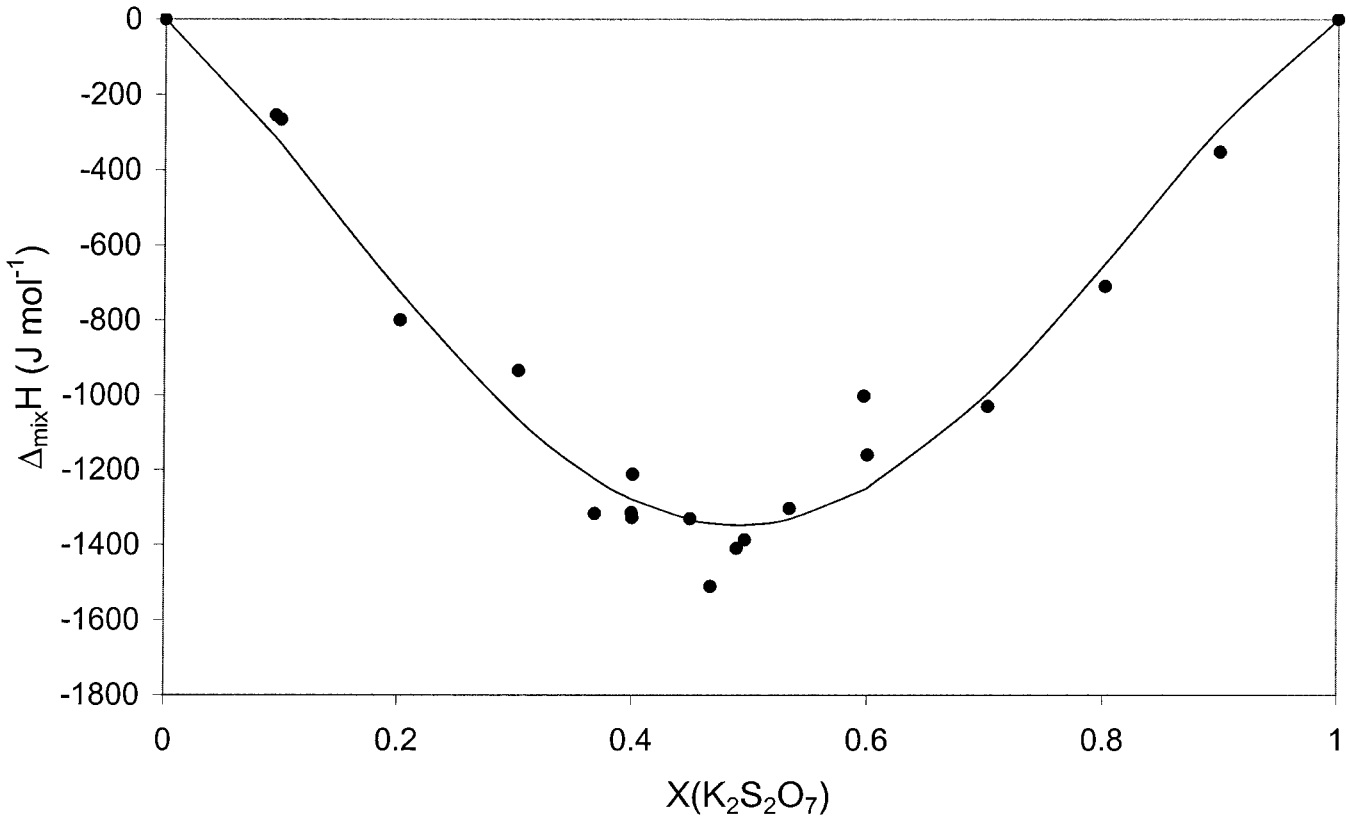


**Figure 4.** Liquid−liquid molar enthalpies of mixing, $\Delta_{mix}H$, of the $Na_2S_2O_7-K_2S_2O_7$ system at 718 K.

observed temperatures of transitions are displayed in Figure 3 together with points taken from the previously[9] published diagram based on solely thermal measurements. A very good accordance is observed between the two methods of investigation. The melting temperatures of the two components previously[16] found to be 675 and 692 K for $Na_2S_2O_7$ and $K_2S_2O_7$,

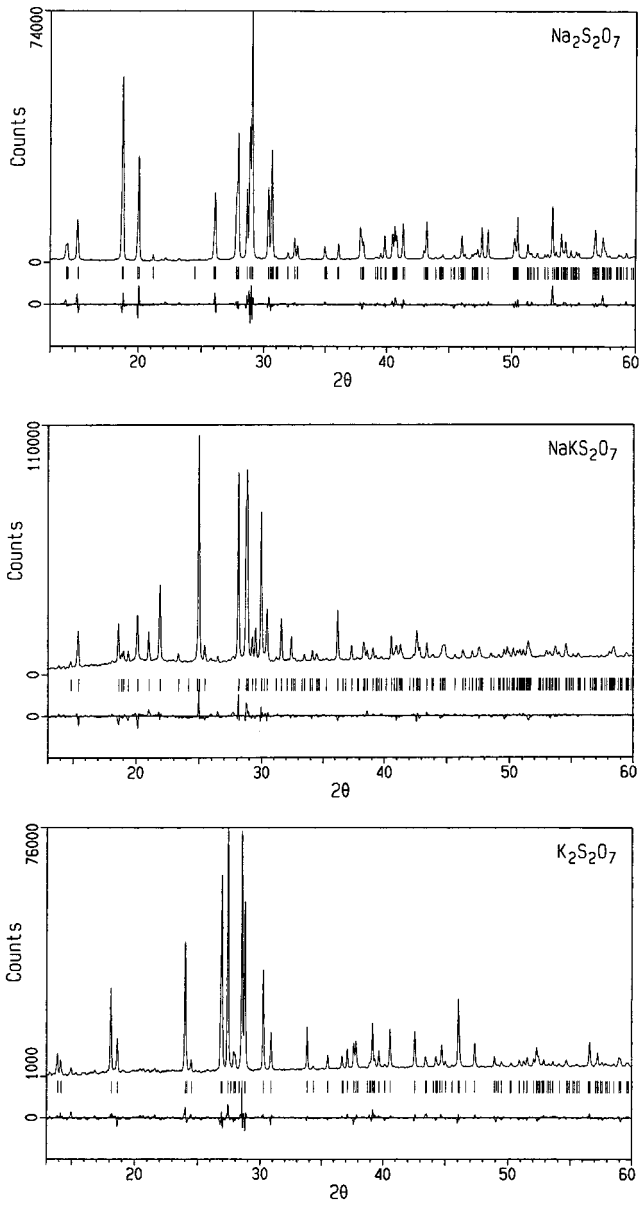


**Figure 5.** Observed and final difference powder diffraction patterns of $Na2S_2O_7$, $NaKS_2O_7$, and $K_2S_2O_7$. Vertical bars indicate the positions of Bragg reflections.

respectively, are confirmed by the present investigation. Also, our previously[5] determined temperature of fusion of 651 K for the 80% $K_2S_2O_7$−20% $Na_2S_2O_7$ mixture agrees very well with 652 K found here for $X_{K_2S_2O_7} = 0.8$.

The maximum found in the diagram at $X_{K_2S_2O_7} = 0.5$ corresponds to the formation of the compound $NaKS_2O_7$ with a melting temperature of 619 K. Further, two eutectics are found close to $X_{K_2S_2O_7} = 0.4$ and 0.6 with temperatures of fusion around 615 and 613 K, respectively. These values are considerably higher, i.e., around 70 K than found in a later published diagram[10] of the binary $Na_2S_2O_7$−$K_2S_2O_7$ system, indicating that in that work the hygroscopic pyrosulfates have been seriously contaminated by hydrogen sulfates.

Some liquidus points in the diagram have been confirmed by our DEA measurements as shown in Figure 3.

In the present work, the enthalpy of liquid−liquid mixing of $Na_2S_2O_7$ and $K_2S_2O_7$ has been measured at 718 K for 18 different compositions. The results are displayed in Figure 4 together with the curve based on the least-squares fit polynomial

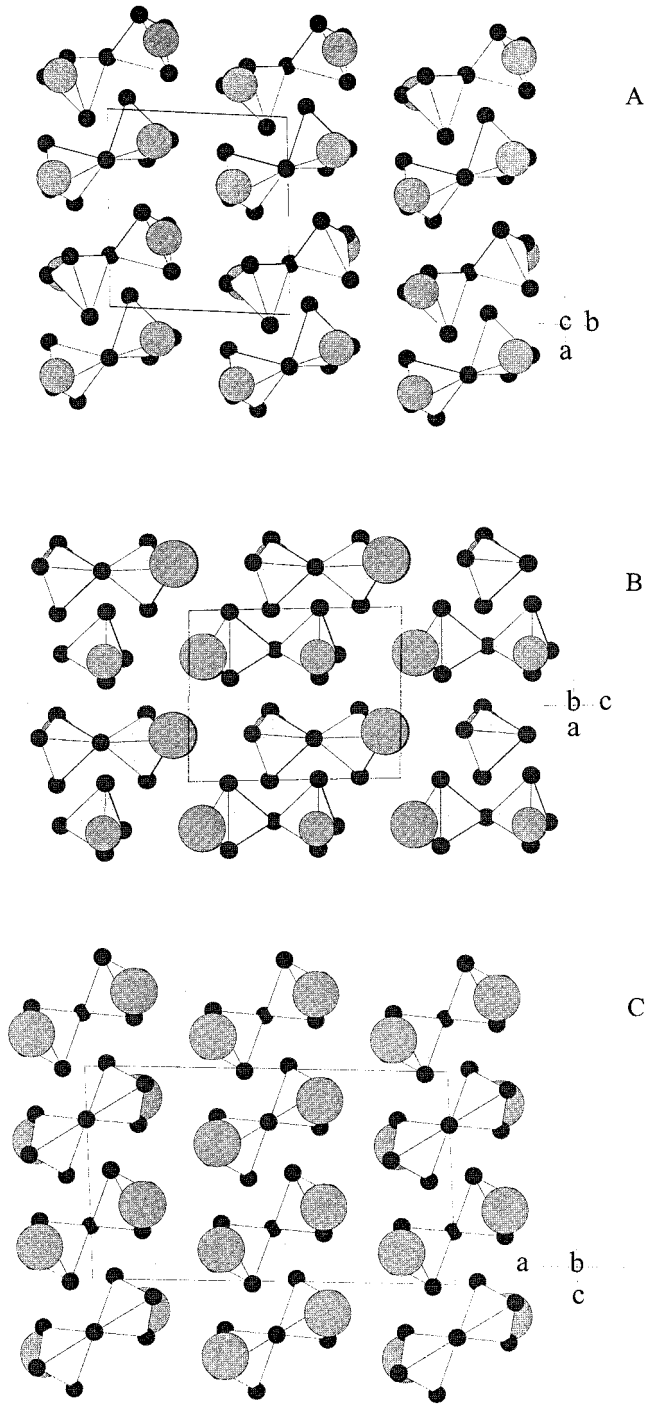


**Figure 6.** Crystal packing of $K_2S_2O_7$ (A), $Na_2S_2O_7$ (B), and $NaKS_2O_7$ (C): small circles, O; medium circles, Na; large circles, K. For convenience, S is not shown.

$$\Delta H_{mix} = x(1-x)(-2.007 \times 10^3 - (1.286 \times 10^4)x + (1.220 \times 10^4)x^2)$$

where $x$ is equal to $X_{K_2S_2O_7}$. The plot exhibits a minimum around $X_{K_2S_2O_7} = 0.5$ of − 1.4 kJ/mol, a rather small value, indicating almost ideal mixing of the liquid pyrosulfates.

In the phase diagram in Figure 3 are the solid−solid transition temperatures found previously[9] given as well. On the basis of the experimental heat of mixing, the heats and temperatures of fusion, and the heat capacities of the solid and liquid pyrosulfates earlier obtained by us,[16] it has been possible to calculate the solid−liquid and solid−solid phase transition temperatures in the whole composition range. A classic method has been used

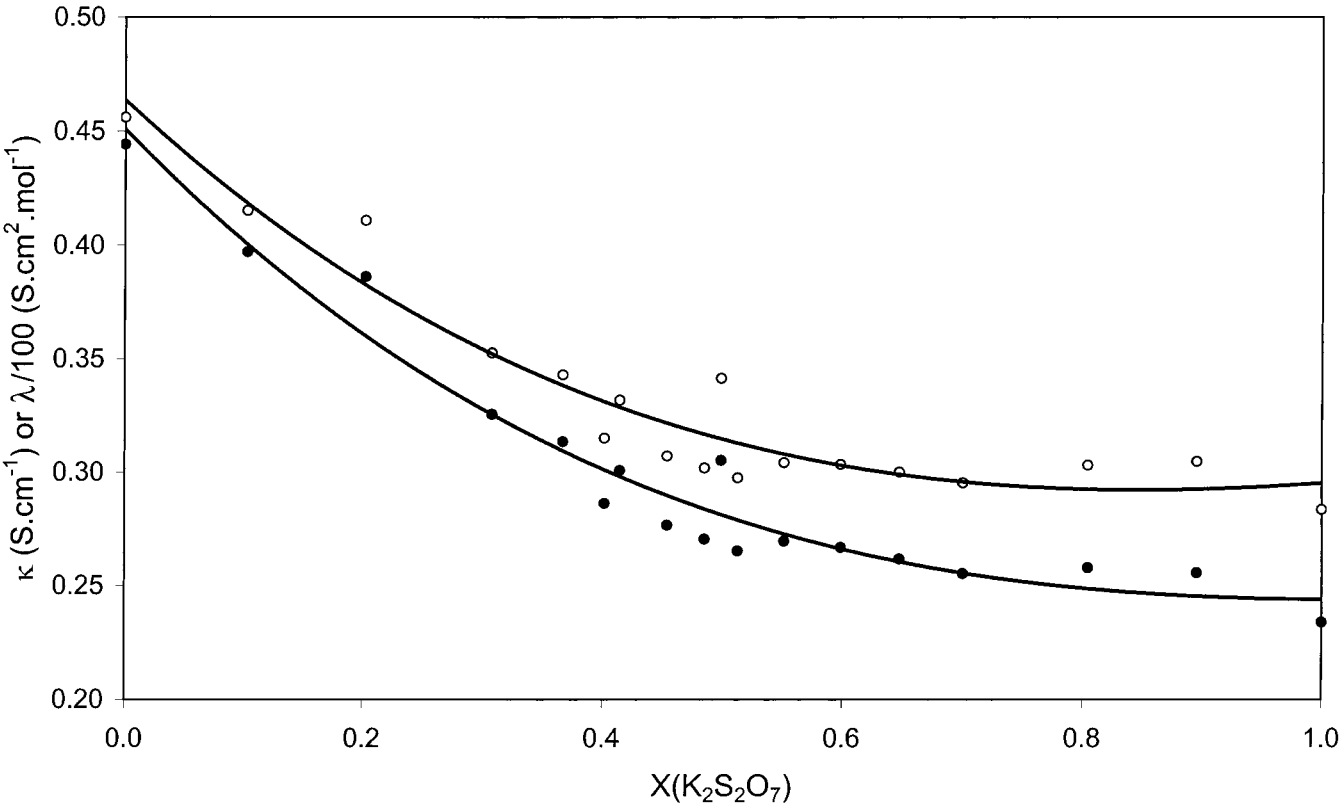


**Figure 7.** Isoterms for $\kappa$ (closed circles) and $\lambda$ (open circles) of the $Na_2S_2O_7-K_2S_2O_7$ molten system at 693 K.

for optimization of the thermodynamic functions. It is based on the equality of the chemical potentials of the two components A ($K_2S_2O_7$) and B ($Na_2S_2O_7$). From these relations we obtain

$$-\Delta G^0_{\mathrm{fus,T}}(\mathrm{A}) = RT\ln[x_{\mathrm{A}}(1)] - RT\ln[x_{\mathrm{A}}(\mathrm{s})] + \bar{G}^{\mathrm{xs}}(\mathrm{A},1) - \bar{G}^{\mathrm{xs}}(\mathrm{A},\mathrm{s}) \quad (1)$$

where $x_{\mathrm{A}}$ and $\bar{G}^{\mathrm{xs}}$ denote, respectively, the molar fraction and excess molar Gibbs free energy of component A. The same relationship is obtained for B. In this calculation, we assume that the excess Gibbs free energy of the solid solution is equal to zero in the whole concentration range. The Gibbs free enthalpy of melting of $K_2S_2O_7$ or $Na_2S_2O_7$ can be deduced at all temperatures from the enthalpy and temperature of melting at the melting point and from the heat capacities (solid and liquid). All these data have been measured by us[16] as mentioned above. In the solid solution rich in $K_2S_2O_7$, for example, the crystal structure of $Na_2S_2O_7$ is the same as $K_2S_2O_7$ and therefore different from the crystal structure of pure $Na_2S_2O_7$. The Gibbs free enthalpy of melting $Na_2S_2O_7$ in the crystal structure of $K_2S_2O_7$ is impossible to obtain experimentally and this function must be calculated. The same conclusion is obtained for $K_2S_2O_7$ in the solid solution rich in $Na_2S_2O_7$. Finally, the assessment of the system is obtained by using all the experimental data and we calculate the following items:

(1) The Gibbs free energy of fusion of $Na_2S_2O_7$ in the crystal structure of $K_2S_2O_7$: $G^*_{\mathrm{fus(Na2S2O7,T)}} = A + BT$; $A = -15.847$ kJ·mol$^{-1}$, $B = 0.057$ kJ·mol$^{-1}$·K$^{-1}$.

(2) The Gibbs free energy of fusion of $K_2S_2O_7$ in the crystal structure of $Na_2S_2O_7$: $G^*_{\mathrm{fus(K2S2O7,T)}} = A' + B'T$; $A' = -35.083$ kJ·mol$^{-1}$; $B' = 0.712$ kJ·mol$^{-1}$·K$^{-1}$.

(3) The excess entropy of the liquid solution: $S^{\mathrm{xs}} = x(1-x)(a+bx)$, where $x = X_{K_2S_2O_7}$, $a = 13.409$ J·mol$^{-1}$·K$^{-1}$, $b = -3.097$ J·mol$^{-1}$.

(4) The enthalpy of formation of the compound $NaKS_2O_7$: $\Delta H^{\mathrm{f}} = -4012$ J·mol$^{-1}$.

(5) The correlation coefficient: 0.999998.

From the thermodynamic functions of this binary system, we have calculated the phase diagram. The result is shown in Figure 3 together with our experimental points and those of others.[9]

**XRD Investigations.** The $Na_2S_2O_7-K_2S_2O_7$ phase diagram suggests the presence of three solid phases at room temperature: $Na_2S_2O_7$, $NaKS_2O_7$, and $K_2S_2O_7$. The crystal structure is only known[17] for $K_2S_2O_7$, while the $Na_2S_2O_7$ phase has been investigated by XRD and indexed.[18] The X-ray powder diffractograms of the pure components and of the 1:1 $Na_2S_2O_7-K_2S_2O_7$ mixture after cooling of the melt are shown in Figure 5. From this, the crystal structure[17] of $K_2S_2O_7$ was confirmed and refined and also the previously reported triclinic unit cell of $Na_2S_2O_7$ was confirmed. The unknown crystal structure of this salt could be solved using EXPO,[19] and it was found to belong to the space group $P$-1 with $a = 6.8037(1)$ Å, $b = 6.8265(1)$ Å, $c = 6.7846(1)$ Å, $\alpha = 116.361(1)°$, $\beta = 95.959(1)°$, $\gamma = 84.194(1)°$, and $Z = 2$. The compound $NaKS_2O_7$ was indexed using TREOR[20] and the structure solved on the basis of a transformation of the $K_2S_2O_7$ structure and a very restrained Rietveld refinement. It belongs also to the space group $P$-1 with $a = 5.9050(1)$ Å, $b = 7.2011(1)$ Å, $c = 7.4190(1)$ Å, $\alpha = 101.707(1)°$, $\beta = 90.696(1)°$, $\gamma = 94.241(1)°$, and $Z = 2$. Despite an apparent similarity between the three solid structures, the differences are large enough to exclude a simple solid solution of the two components of the binary system (Figure 5).

The crystal structures of $Na_2S_2O_7$ and $NaKS_2O_7$ are shown in Figure 6. The stacking sequences show a similar arrangement for the Na−Na and K−K structures while the Na−K structure exhibits a zigzaging pyrosulfate stacking. The smaller Na-ions allow a closer packing of the pyrosulfates than the K-ions. In

fact, the densities of the three phases increases in going from K−K over Na−K to Na−Na, calculated to be 2.568, 2.570, and 2.633 g/cm$^3$, respectively.

**Conductivity of the Liquid $Na_2S_2O_7$−$K_2S_2O_7$ System.** The conductivities of the 18 different compositions measured in the liquid region have been fitted as previously[7] to polynomials of the form $\kappa = A(x) + B(x)(T - T_m) + C(x)(T - T_m)^2$ where $T \geq T_{liquidus}$ and $T_m$ is the middle temperature as given in Table 1. The conductivity isoterm at 693 K for all of the measured compositions is displayed in Figure 7 together with the molar conductivity of the melt, $\lambda = kV^M$, that has been calculated based on the previously published[16] densities giving the molar volume of the melt, $V^M$, at any composition, and assuming ideal mixing of $Na_2S_2O_7$ and $K_2S_2O_7$.

The conductivity of $Na_2S_2O_7$(l) and $K_2S_2O_7$(l) measured here compares very well (within approximately 1%) with our previously measured values,[16] calculated at 688 and 723 K for the two salts, respectively. The least-squares fit to the data points $\kappa = 0.4510 - 0.5358x + 0.4550x^2 - 0.1261x^3$ ($x = X_{K_2S_2O_7}$) shows a steady decrease with increasing content of $K_2S_2O_7$ in the melt, as is the case also for the molar conductivity of the melt, $\lambda = 0.4637 - 0.4815x + 0.4198x^2 - 0.1069x^3$. This indicates that the conductivity of the melt decreases by increasing displacement of the smaller and more mobile $Na^+$ ion by the larger $K^+$ ion, as expected. This tendency was also observed earlier by us[3] for the row $Na^+$, $K^+$, $Rb^+$, and $Cs^+$ based on the conductivities of the alkali pyrosulfates at 753 K.

**Relation to Catalysis.** The "classical" industrial $SO_2$ oxidation catalyst is based on a mixture of K and Na salts as promoters for the active component, $V_2O_5$. Usually, the composition range of K is 70−90% and Na accordingly 30−10%. On the basis of our phase diagram, the temperature of fusion decreases from about 690 to 630 K in going from pure $K_2S_2O_7$ to the 70% $K_2S_2O_7$−30% $Na_2S_2O_7$ mixture. Thus an appreciable decrease of the liquidus temperature of the catalyst solvent system is obtained by mixing the two alkali promoters. Previously,[5] we have constructed the phase diagram of the pseudo binary catalyst model system (80% $K_2S_2O_7$−20% $Na_2S_2O_7$)−$V_2O_5$ and an eutectic with composition $X_{V_2O_5} = 0.175$ and a melting temperature of 587 K was found. Therefore, on the basis of the present study an even lower temperature of fusion is expected for the eutectic of the pseudobinary system comprising the 60% $K_2S_2O_7$−40% $Na_2S_2O_7$ (eutectic mixture (Figure 3), mp 613 K) and $V_2O_5$, possibly as low as 575 K. Thus, the desired low-melting $SO_2$ oxidation catalyst might be manufactured based on this solvent system. However other factors as the stability of the catalytical active V(V) complexes[21] and the solubility of the V(IV) complexes[22] formed by reduction of V(V) by the $SO_2$ containing synthesis gas have to be considered as well, as should the influence of the solvent composition on the diffusion resistance for the gaseous reactants and products.

**Acknowledgment.** This investigation has been supported by the Danish Natural Science Foundation, the French Ministry of Foreign Affairs, and the NATO Science for Peace Program (SfP971984).

## References and Notes

(1) Topsøe, H. F. A.; Nielsen, A. *Trans. Dan. Akad. Technol. Sci.* **1947**, *1*, 18.
(2) Folkmann, G. E.; Eriksen, K. M.; Fehrmann, R.; Gaune-Escard, M.; Hatem, G.; Lapina, O. B.; Terskikh, V. *J. Phys. Chem. B* **1998**, *102*, 24.
(3) Abdoun, F.; Hatem, G.; Gaune-Escard, M.; Eriksen, K. M.; Fehrmann, R. *J. Phys. Chem. B* **1999**, *103*, 3559.
(4) Folkmann, F. E.; Hatem, G.; Fehrmann, R.; Gaune-Escard, M.; Bjerrum, N. J. *Inorg. Chem.* **1991**, *30*, 4057
(5) Karydis, D. A.; Boghosian, S.; Fehrmann, R. *J. Catal.* **1994**, *145*, 312.
(6) Hatem, G.; Gaune-Escard, M.; Rasmussen, S. B.; Fehrmann, R. *J. Phys. Chem. B* **1999**, *103*, 1027.
(7) Eriksen, K. M.; Fehrmann, R.; Hatem, F.; Gaune-Escard, M.; Lapina, O. B.; Mastikhin, V. M. *J. Phys. Chem. B* **1996**, *100*, 10771.
(8) Manuscript in preparation.
(9) Colombier, M.; Said, J.; Leclerq, P.; Cohen-Adad, R. *Rev. Chim. Miner.* **1981**, *18*, 162.
(10) Gubareva, V. N.; Bel'skaya, N. P.; Pogodilova, E. G.; Borisov, V. M.; Stahl, R. M. *Zh. Prikl. Khim.* **1988**, *61*, 1377.
(11) Boghosian, S.; Fehrmann, R.; Bjerrum, N. J.; Papatheodorou, G. N. *J. Catal.* **1989**, *119*, 121.
(12) Hatem, G.; Fehrmann, R.; Gaune-Escard, M.; Bjerrum, N. J. *J. Phys. Chem.* **1987**, *91*, 195.
(13) Gaune-Escard, M.; Bros, J. P. *Thermochim. Acta* **1978**, *31*, 323.
(14) Cerenius, Y.; Ståhl, K.; Svensson, L. A.; Ursby, T.; Oskarsson, Å.; Albertsson, J.; Liljas, A. *J. Synchr. Rad.* **2000**, *7*, 203.
(15) Ståhl, K. *J. Appl. Crystallogr.* **2000**, *33*, 394.
(16) Hatem, G.; Abdoun, F.; Gaune-Escard, M.; Eriksen, K. M.; Fehrmann, R. *Thermochim. Acta* **1998**, *319*, 33.
(17) Lynton, H.; Truter, M. R. *J. Chem. Soc.* **1960**, 5112.
(18) Sonneveld, E., JCPDS-ICDD Powder pattern 42-0692, 1991.
(19) Altomare, A.; Burla, M. C.; Cascarano, G.; Giacovazzo, C.; Guagliardi, A.; Moliterni, A. G. G.; Polidori, G. *J. Appl. Crystallogr.* **1995**, *28*, 842. Altomare, A.; Cascarano, G.; Giacovazzo, C.; Burla, M. C.; Polidori, G.; Camalli, M. *J. Appl. Crystallogr.* **1994**, *27*, 435.
(20) Werner, P. E.; Eriksson, L.; Westdahl, M. *J. Appl. Crystallogr.* **1985**, *18*, 367.
(21) Lapina, O. B.; Bal'zhinimaev, B. S.; Boghosian, S.; Eriksen, K. M.; Fehrmann, R. *Catal. Today* **1999**, 51, 469.
(22) Eriksen, K. M.; Karydis, D. A.; Boghosian, S.; Fehrmann, R. *J. Catal.* **1995**, 155, 32.